

Trapped surfaces in a hadronic fluid

Neven Bilić and Dijana Tolić

Rudjer Bošković Institute,

P.O. Box 180, 10001 Zagreb, Croatia

E-mail: bilic@thphys.irb.hr, dijana.tolic@irb.hr

August 7, 2018

Abstract

Pion propagation in a hadronic fluid with a nonhomogeneous relativistic flow is studied in terms of the linear sigma model. The wave equation turns out to be equivalent to the equation of motion for a massless scalar field propagating in a curved spacetime geometry. The metric tensor depends locally on the soft pion dispersion relation and the four-velocity of the fluid. For a relativistic flow in curved spacetime the apparent and trapping horizons may be defined in the same way as in general relativity. An expression for the analog surface gravity is derived.

1 Introduction

In current understanding the matter created in heavy ion collisions behaves as a nearly perfect expanding fluid [1] under extreme conditions of very high density and temperature. This hydrodynamic behavior was observed at Brookhaven's Relativistic Heavy Ion Collider (RHIC) and recently confirmed by the ALICE collaboration in Pb-Pb collisions at the LHC [2, 3]. In high energy collisions the produced particles are predominantly pions. The agreement between the pion production results reported in [2] and the theoretical hydrodynamical model predictions [4] is truly remarkable. A realistic hydrodynamic model may be constructed [5] in which a transverse expansion is superimposed on a longitudinal boost invariant expansion [6].

It is often stated by particle physicists that heavy ion collisions create mini big bangs¹ – events in which matter is created under extreme conditions of high density and high temperature resembling the conditions in the early Universe a fraction of a second after the big bang. The expansion of hadronic matter that takes place immediately after a heavy ion collision has certain similarity with the cosmological expansion. However, the analogy is rather superficial since in a cosmological expansion of spacetime after the big bang the gravity

¹A few recent quotations from the press: “What we’re doing is reproducing the conditions that existed at the very early Universe, a few millionths of a second after the big bang” [7]. “The Large Hadron Collider has successfully created a ‘mini-big bang’ by smashing together lead ions instead of protons” [8]. “The collisions generated mini big bangs and the highest temperatures and densities ever achieved in an experiment” [9].

plays the essential role, whereas high energy collisions and subsequent expansion does not involve gravity at all. Although the Minkowski spacetime with expanding hadronic matter can be mapped into an expanding spacetime, the resulting spacetime is still flat. However, we will demonstrate here that in high energy collisions a much closer analogy with cosmology may be drawn owing to the effective analog gravity with essentially curved geometry. Various aspects of analog gravity (for a review and extensive list of references see [10]) have been studied in acoustics [11] optics [12], superfluidity [13], black hole accretion [14, 15], and hadronic fluid near the QCD chiral phase transition [16]. In this paper we study in detail the framework of analog gravity provided by a hadronic fluid at nonzero temperature for the whole range of temperatures below the chiral phase transition. We show that the analog cosmological spacetime corresponds to a contracting Friedmann-Robertson-Walker (FRW) universe with a nontrivial apparent horizon.

Strongly interacting matter is described at the fundamental level by a non-Abelian gauge theory called quantum chromodynamics (QCD). At large distances or small momenta, QCD exhibits the phenomena of quark confinement and chiral symmetry breaking. At low energies, the QCD vacuum is characterized by a nonvanishing expectation value [17]: $\langle\bar{\psi}\psi\rangle\approx(235\text{ MeV})^3$, the so-called quark condensate, which describes the density of quark-antiquark pairs found in the QCD vacuum and its nonvanishing value is the manifestation of chiral symmetry breaking. The phenomenological importance of the chiral transition and possible experimental signatures have been discussed by Harris and Müller [18].

The chiral symmetry breaking and restoration at finite temperature may be conveniently studied using the linear sigma model [19, 20] originally proposed as a model for strong nuclear interactions [21]. Today, the linear sigma model serves as an effective model for the low energy (low temperature) phase of QCD. The basic model involves four scalar fields (three pions and a sigma meson) and two-flavor constituent quarks. In the chirally symmetric phase at temperatures above the chiral transition point the mesons are massive with equal masses and quarks are massless. In the chirally broken phase the pions are massless, whereas the quarks and sigma meson acquire a nonzero mass proportional to the chiral condensate. At temperatures below the chiral phase transition point the pions, although they are massless, propagate slower than light [22, 23, 24] with a velocity approaching zero at the critical temperature. Hence, it is very likely that there exists a region where the flow velocity exceeds the pion velocity and the analog trapped region may form. In our previous paper [16] we demonstrated that a region containing analog trapped surfaces forms near the chiral phase transition. The purpose of this paper is to study general conditions for the formation of a trapped region with the inner boundary as a marginally trapped surface which we refer to as the *analog apparent horizon*. Our approach is based on the linear sigma model combined with a boost invariant Bjorken type spherical expansion. A similar model has been previously studied in the context of disoriented chiral condensate [25].

The remainder of the paper is organized as follows. In Sec. 2 we describe the properties and the dynamics of the chiral fluid at finite temperature. The analog geometry of the expanding chiral fluid is studied in Sec. 3 in which we derive the condition for the analog apparent horizon and study the analog Hawking effect. In the concluding section, Sec. 4, we summarize our results and discuss physical consequences. Finally, in the Appendix A we outline basic notions related to trapped surfaces in black hole physics and cosmology.

2 Chiral fluid

In this section we focus on the physics of hadrons at finite temperature and study the properties and the dynamics of an expanding chiral fluid. We base our study on a linear sigma model with no fermions which we describe in Sec. 2.1. In Sec. 2.2 we calculate the effective velocity of pions propagating in a chiral medium. We model the fluid expansion on a boost invariant spherical expansion of the Bjorken type which we describe in Sec. 2.3

2.1 Linear sigma model

Consider a linear sigma model at finite temperature in a general curved spacetime background. For our purpose it is sufficient to study the model with no constituent fermions. The thermal bath provides a medium which may have an inhomogeneous velocity field. The dynamics of mesons in such a medium is described by an effective chirally symmetric Lagrangian of the form [26]

$$\mathcal{L} = \frac{1}{2}(a g^{\mu\nu} + b u^\mu u^\nu) \partial_\mu \varphi \partial_\nu \varphi - \frac{m_0^2}{2} \varphi^2 - \frac{\lambda}{4} (\varphi^2)^2, \quad (1)$$

where u_μ is the velocity of the fluid, and $g_{\mu\nu}$ is the background metric. The mesons $\varphi \equiv (\sigma, \boldsymbol{\pi})$ constitute the $(\frac{1}{2}, \frac{1}{2})$ representation of the chiral $SU(2) \times SU(2)$. The parameters a and b depend on the local temperature T and on the parameters of the model m_0 and λ and may be calculated in perturbation theory. At zero temperature the medium is absent in which case $a = 1$ and $b = 0$.

If $m_0^2 < 0$ the chiral symmetry will be spontaneously broken. At the classical level, the σ and π fields develop nonvanishing expectation values such that at zero temperature

$$\langle \sigma \rangle^2 + \langle \boldsymbol{\pi} \rangle^2 = -\frac{m_0^2}{\lambda} \equiv f_\pi^2. \quad (2)$$

It is convenient to choose here

$$\langle \pi_i \rangle = 0, \quad \langle \sigma \rangle = f_\pi. \quad (3)$$

At nonzero temperature the expectation value $\langle \sigma \rangle$ is temperature dependent and vanishes at the chiral transition point. Redefining the fields

$$\varphi \rightarrow \varphi + \varphi'(x) = (\sigma, \boldsymbol{\pi}) + (\sigma'(x), \boldsymbol{\pi}'(x)), \quad (4)$$

where $\boldsymbol{\pi}'$ and σ' are quantum fluctuations around the constant values $\boldsymbol{\pi} = 0$ and $\sigma = \langle \sigma \rangle$, respectively, we obtain the effective Lagrangian in which the chiral symmetry is explicitly broken:

$$\mathcal{L}' = \frac{1}{2}(a g^{\mu\nu} + b u^\mu u^\nu) \partial_\mu \varphi' \partial_\nu \varphi' - \frac{m_\sigma^2}{2} \sigma'^2 - \frac{m_\pi^2}{2} \boldsymbol{\pi}'^2 - g \sigma' \varphi'^2 - \frac{\lambda}{4} (\varphi'^2)^2. \quad (5)$$

The fields σ' and $\boldsymbol{\pi}'$ correspond to the physical sigma meson and pions, respectively. The effective masses and the trilinear coupling g are functions of σ defined as

$$\begin{aligned} m_\sigma^2 &= m_0^2 + 3\lambda\sigma^2, \\ m_\pi^2 &= m_0^2 + \lambda\sigma^2, \\ g &= \lambda\sigma. \end{aligned} \quad (6)$$

For temperatures below the chiral transition point the meson masses are given by

$$m_\pi^2 = 0; \quad m_\sigma^2 = 2\lambda\sigma^2, \quad (7)$$

in agreement with the Goldstone theorem. The temperature dependence of the chiral condensate σ is obtained by minimizing the thermodynamical potential $\Omega = -(T/V) \ln Z$ with respect to σ at fixed inverse temperature β . At one loop order, the extremum condition reads [20]

$$\sigma^2 = f_\pi^2 - 3 \int \frac{d^3p}{(2\pi)^3} \frac{1}{\omega_\sigma} n_B(\omega_\sigma) - 3 \int \frac{d^3p}{(2\pi)^3} \frac{1}{\omega_\pi} n_B(\omega_\pi), \quad (8)$$

where

$$\omega_\pi = |\mathbf{p}|; \quad \omega_\sigma = (\mathbf{p}^2 + m_\sigma^2)^{1/2} \quad (9)$$

are the energies of the π and σ particles, respectively, and

$$n_B(\omega) = \frac{1}{e^{\beta\omega} - 1} \quad (10)$$

is the Bose-Einstein distribution function. Equation (8) has been derived from the zero order thermodynamical potential with meson masses at one loop order [20]. This approximation corresponds to the leading order in $1/N$ expansion, where N is the number of scalar fields [27]. In our case, $N = 4$. The right-hand side of (8) depends on σ through the mass m_σ given by (7). The behavior of σ near the critical temperature should be analyzed with special care. A straightforward solution to (8) as a function of temperature exhibits a weak first order phase transition [20, 28]. However, Pisarski and Wilczek have shown on general grounds that the phase transition in $SU(2) \times SU(2)$ chiral models should be of second order [29]. Hence, it is generally believed that a first order transition is an artifact of the one loop approximation. Two loop calculations [30] make an improvement and confirm the general analysis of [29]. It is possible to mimic the second order phase transition even with (8) by making the σ -meson mass temperature independent all the way up to the critical temperature and equal to its zero temperature mean field value given by

$$m_\sigma^2 = 2\lambda f_\pi^2, \quad (11)$$

instead of (7). We fix the coupling λ from the values of m_σ and f_π for which we take $m_\sigma = 1$ GeV and $f_\pi = 92.4$ MeV as a phenomenological input. In Fig. 1 we plot the solutions to (8) for both temperature dependent and temperature independent m_σ exhibiting apparent first and second order phase transitions, respectively. In the rest of our paper we employ the solution that corresponds to the second order phase transition. For our choice of parameters we find numerically $T_c = 182.822$ MeV.

The propagation of pions is governed by the equation of motion

$$\frac{1}{\sqrt{-g}} \partial_\mu \left[\sqrt{-g} (a g^{\mu\nu} + b u^\mu u^\nu) \partial_\nu \boldsymbol{\pi} \right] + V(\sigma, \boldsymbol{\pi}) \boldsymbol{\pi} = 0, \quad (12)$$

where

$$V(\sigma, \boldsymbol{\pi}) = m_\pi^2 + g\sigma + \lambda(\sigma^2 + \boldsymbol{\pi}^2) \quad (13)$$

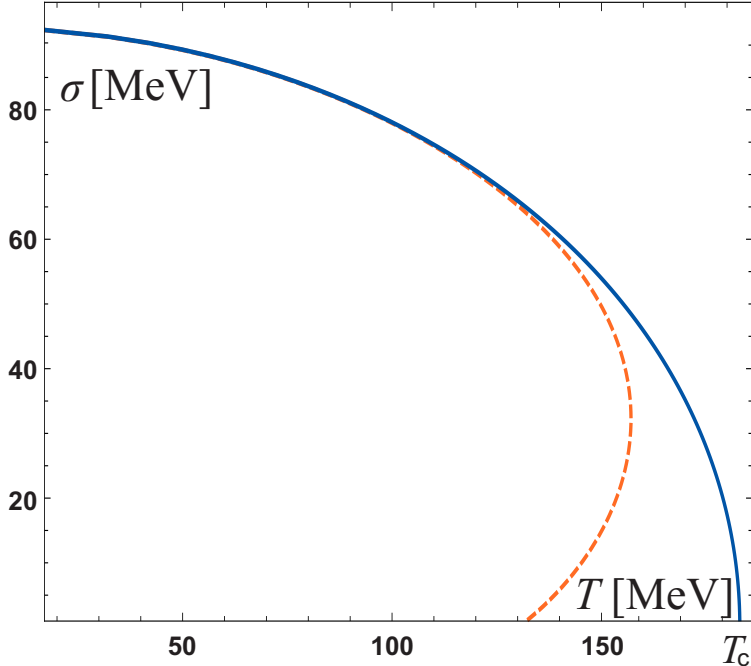


Figure 1: Chiral condensate as a function of temperature for a temperature independent (full line) and temperature dependent m_σ (dashed line), representing a second order phase transition and first order (discontinuous) phase transition, respectively. The critical temperature of the second order phase transition is indicated by T_c .

is the interaction potential. In the comoving reference frame in flat spacetime, Eq. (12) reduces to the wave equation

$$(\partial_t^2 - c_\pi^2 \Delta + \frac{c_\pi^2}{a} V) \boldsymbol{\pi} = 0, \quad (14)$$

where the quantity c_π , defined by

$$c_\pi^2 = \left(1 + \frac{b}{a}\right)^{-1}, \quad (15)$$

is the pion velocity. As we shall demonstrate in the next section, the constants a and b may be derived from the finite-temperature perturbation expansion of the pion self energy.

2.2 Pion velocity

At temperatures below the chiral transition point, the pions are massless. However, the velocity of massless particles in a medium is not necessarily equal to the velocity of light in the chiral fluid pions usually propagate slower than light.² The pion velocity in a sigma

²If the chiral fermions are present, pions become superluminal in certain range of temperature and baryon chemical potential [26].

model at finite temperature has been calculated at one loop level by Pisarski and Tytgat in the low temperature approximation [22] and by Son and Stephanov for temperatures close the chiral transition point [23, 24]. It has been found that the pion velocity vanishes as one approaches the critical temperature. Here we summarize the calculation of the parameters a and b in the entire range of temperatures in the chiral symmetry broken phase [26].

The pion velocity may be derived from the self-energy $\Sigma(q, T)$ in the limit where the external momentum q approaches 0. For a flat background geometry $g_{\mu\nu} = \eta_{\mu\nu}$, the inverse pion propagator Δ^{-1} , derived directly from the effective Lagrangian (5) as

$$\Delta^{-1} = aq^\mu q_\mu + b(q^\mu u_\mu)^2 - m_\pi^2, \quad (16)$$

may in the limit $q \rightarrow 0$ be expressed in the form

$$Z_\pi \Delta^{-1} = q^\mu q_\mu - \frac{1}{2!} q^\alpha q^\beta \left[\frac{\partial}{\partial q^\alpha} \frac{\partial}{\partial q^\beta} (\Sigma(q, T) - \Sigma(q, 0)) \right]_{q=0} + \dots, \quad (17)$$

where the ellipsis denotes the terms of higher order in q^μ . The q^μ independent term of the self-energy absorbs in the renormalized pion mass, equal to zero in the chiral symmetry broken phase. The subtracted $T = 0$ term has been absorbed in the wave function renormalization factor Z_π . By comparing this equation with Eq. (16) written in the comoving frame as

$$\Delta^{-1} = (a + b)q_0^2 - a\mathbf{q}^2 - m_\pi^2, \quad (18)$$

we can express the parameters a and b , and hence the pion velocity, in terms of second derivatives of $\Sigma(q, T)$ evaluated at $q^\mu = 0$. At one loop level the only diagram that gives a nontrivial q dependence of Σ is the bubble diagram. Subtracting the $T = 0$ term one finds [24]

$$\begin{aligned} \Sigma(q) \equiv \Sigma(q, T) - \Sigma(q, 0) &= -4g^2 \int \frac{d^3p}{(2\pi)^3} \frac{1}{2\omega_\pi 2\omega_{\sigma,q}} \\ &\left\{ [n_B(\omega_\pi) + n_B(\omega_{\sigma,q})] \left(\frac{1}{\omega_{\sigma,q} + \omega_\pi} + \frac{1}{\omega_{\sigma,q} + \omega_\pi + q_0} \right) \right. \\ &\left. + [n_B(\omega_\pi) - n_B(\omega_{\sigma,q})] \left(\frac{1}{\omega_{\sigma,q} - \omega_\pi} + \frac{1}{\omega_{\sigma,q} - \omega_\pi + q_0} \right) \right\}, \quad (19) \end{aligned}$$

where $\omega_{\sigma,q} = [(\mathbf{p} - \mathbf{q})^2 + m_\sigma^2]^{1/2}$. Here we take m_σ to be a function of σ through Eq. (7). A straightforward evaluation of the second derivatives of $\Sigma(q)$ at $q_\mu = 0$ yields

$$a = 1 + \frac{16g^2}{m_\sigma^4} \int \frac{d^3p}{(2\pi)^3} \left[\frac{n_B(\omega_\pi)}{4\omega_\pi} + \frac{n_B(\omega_\sigma)}{4\omega_\sigma} - \frac{1}{3} \frac{\omega_\pi^2}{m_\sigma^2} \left(\frac{n_B(\omega_\pi)}{\omega_\pi} - \frac{n_B(\omega_\sigma)}{\omega_\sigma} \right) \right], \quad (20)$$

$$b = \frac{16g^2}{m_\sigma^4} \int \frac{d^3p}{(2\pi)^3} \left[\frac{\omega_\pi n_B(\omega_\pi)}{m_\sigma^2} - \frac{\omega_\sigma n_B(\omega_\sigma)}{m_\sigma^2} + \frac{1}{3} \frac{\omega_\pi^2}{m_\sigma^2} \left(\frac{n_B(\omega_\pi)}{\omega_\pi} - \frac{n_B(\omega_\sigma)}{\omega_\sigma} \right) \right]. \quad (21)$$

The pion velocity c_π as given by (15) depends on temperature explicitly through the thermal distribution function n_B and implicitly through the chiral condensate σ given by Eq. (8). In Fig. 2 we plot c_π as a function of temperature corresponding to two solutions depicted in the left panel.

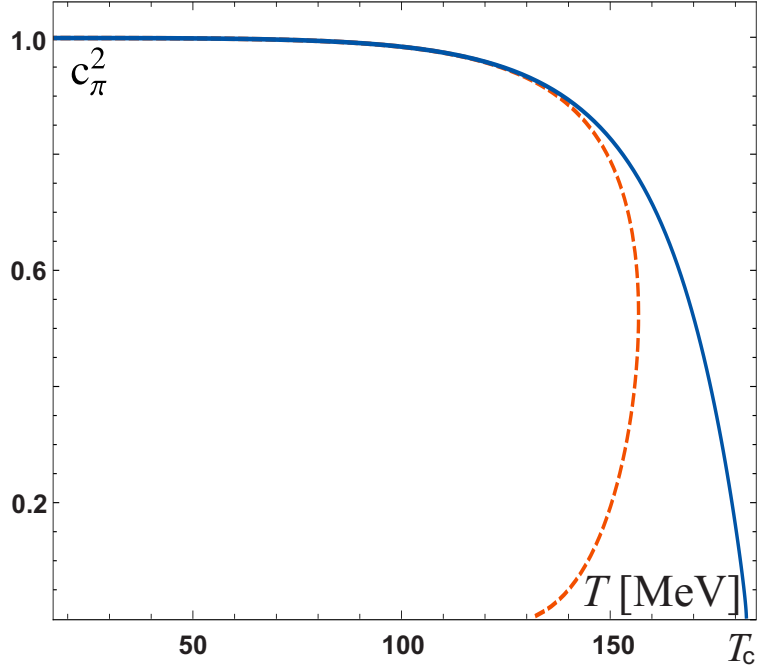


Figure 2: Pion velocity as a function of temperature for a temperature independent (full line) and temperature dependent m_σ (dashed line). The critical temperature of the second order phase transition is indicated by T_c .

2.3 Spherical Bjorken expansion

In order to explore the analogy between the chiral fluid and cosmological expansions, we consider a boost invariant spherically symmetric Bjorken type expansion [6] in Minkowski background spacetime. In radial coordinates $x^\mu = (t, r, \vartheta, \varphi)$, the fluid velocity is given by

$$u^\mu = (\gamma, \gamma v, 0, 0) = (t/\tau, r/\tau, 0, 0), \quad (22)$$

where $v = r/t$ is the radial three-velocity and $\tau = \sqrt{t^2 - r^2}$ is the *proper time*. Using the so-called *radial rapidity*

$$y = \frac{1}{2} \ln \frac{t+r}{t-r}, \quad (23)$$

the velocity is expressed as

$$u^\mu = (\cosh y, \sinh y, 0, 0), \quad (24)$$

and hence, the radial three-velocity is

$$v = \tanh y. \quad (25)$$

It is convenient to change $(t, r, \vartheta, \varphi)$ to new coordinates $(\tau, y, \vartheta, \varphi)$ via the transformation

$$\begin{aligned} t &= \tau \cosh y, \\ r &= \tau \sinh y. \end{aligned} \quad (26)$$

In these coordinates the background Minkowski metric takes the form

$$g_{\mu\nu} = \begin{pmatrix} 1 & & & \\ & -\tau^2 & & \\ & & -\tau^2 \sinh^2 y & \\ & & & -\tau^2 \sinh^2 y \sin^2 \vartheta \end{pmatrix}. \quad (27)$$

and the velocity components become $u^\mu = (1, 0, 0, 0)$. Hence, the new coordinate frame is comoving. The metric (27) corresponds to the Milne cosmological model – a homogeneous, isotropic, expanding universe with the cosmological scale $a = \tau$ and negative spatial curvature.

The functional dependence of T on τ follows from the energy-momentum conservation. For a perfect relativistic fluid the energy-momentum tensor is given by

$$T_{\mu\nu} = (p + \rho)u_\mu u_\nu - pg_{\mu\nu}, \quad (28)$$

where p and ρ denote, respectively, the pressure and the energy density of the fluid. From the energy-momentum conservation

$$T^{\mu\nu}{}_{;\nu} = 0 \quad (29)$$

applied to (28) we find

$$u^\mu \rho_{;\mu} + (p + \rho)u^\mu{}_{;\mu} = 0, \quad (30)$$

where the subscript $;\mu$ denotes the covariant derivative associated with the background metric. Since our fluid is dominated by massless pions at nonzero temperature, it is a reasonable approximation to assume the equation of state $p = \rho/3$ of an ideal gas of massless bosons. Then, Eq. (30) in comoving coordinates reads

$$\frac{\partial \rho}{\partial \tau} + \frac{4\rho}{\tau} = 0 \quad (31)$$

with the solution

$$\rho = \rho_0 \left(\frac{\tau_0}{\tau} \right)^4. \quad (32)$$

This expression combined with the density of the pion gas [31]

$$\rho = \frac{\pi^2}{10} T^4, \quad (33)$$

implies the temperature profile

$$T = T_0 \frac{\tau_0}{\tau}. \quad (34)$$

The constants T_0 and τ_0 may be fixed from the phenomenology of high energy collisions. For example, if we choose $T_0 = 1\text{GeV}$, then a typical value of $\rho = 1\text{GeV}/\text{fm}^3$ at $\tau \approx 5\text{fm}$ [32] is obtained with $\tau_0 = 1.5\text{fm}$. In our case, with these values the interesting range of temperatures T between 100 and 200 MeV corresponds to τ between 15 and 30 fm. In the following we work with $T_0 = 1\text{GeV}$ and keep τ_0 unspecified so that physical quantities of dimension of time or length are expressed in units of τ_0 .

3 Analog cosmology

In this section we turn to study the analog metric and formation and properties of the apparent horizon in an expanding chiral fluid. To this end we outline the formalism in the first subsection and derive a condition for the apparent horizon for a general hyperbolic spacetime. In Sec. 3.2 we derive the analog metric for the expanding chiral fluid and study the properties of the analog apparent horizon. Then, in Sec. 3.3 we exploit the Kodama-Hayward definition of surface gravity to derive the Hawking temperature as a function of the parameters of the chiral fluid, in particular, as a function of the local fluid temperature.

3.1 Radial null geodesics

To study the apparent horizon in an expanding chiral fluid we need to examine the behavior of radial null geodesics of the analog metric which we shall derive in Sec. 3.2. With hindsight, we first consider a spacetime of the form

$$ds^2 = \beta(\tau)^2 d\tau^2 - \alpha(\tau)^2 (dy^2 + \sinh^2 y d\Omega^2), \quad (35)$$

where β and α are arbitrary functions of τ . The metric tensor is

$$G_{\mu\nu} = \begin{pmatrix} \beta^2 & & & \\ & -\alpha^2 & & \\ & & -\alpha^2 \sinh^2 y & \\ & & & -\alpha^2 \sinh^2 y \sin^2 \vartheta \end{pmatrix}. \quad (36)$$

This metric represents the class of hyperbolic ($k = -1$) FRW spacetimes including the flat spacetime example (27). We denote by l_+^μ and l_-^μ the vectors tangent to outgoing and ingoing affinely parametrized radial null geodesics normal to a spherical two-dimensional surface S . The tangent vectors are null with respect to the metric (36), i.e.,

$$G_{\mu\nu} l_+^\mu l_+^\nu = G_{\mu\nu} l_-^\mu l_-^\nu = 0. \quad (37)$$

Using the geodesic equation

$$l^\mu \nabla_\mu l^\nu = 0, \quad (38)$$

where the symbol ∇_μ denotes the covariant derivative associated with the metric (36), one easily finds the tangent null vectors corresponding to four types of radial null geodesics,

$$l_\pm^\mu = q_\pm \alpha^{-1} (\beta^{-1}, \pm \alpha^{-1}, 0, 0), \quad (39)$$

tangent to future directed and

$$l_\pm^\mu = \tilde{q}_\pm \alpha^{-1} (-\beta^{-1}, \pm \alpha^{-1}, 0, 0), \quad (40)$$

to past directed null geodesics, where q_+ , q_- , \tilde{q}_+ , and \tilde{q}_- are arbitrary positive constants. The corresponding affine parameters λ_+ and λ_- for the outgoing and ingoing null geodesics, respectively, are found to satisfy

$$\frac{d\lambda_\pm}{d\tau} = \frac{1}{q_\pm} \alpha \beta \quad (41)$$

for future directed and

$$\frac{d\lambda_{\pm}}{d\tau} = -\frac{1}{\tilde{q}_{\pm}}\alpha\beta, \quad (42)$$

for past directed null geodesics. For simplicity, from now on we set $q_+ = q_- = \tilde{q}_+ = \tilde{q}_- = 1$.

The null vectors l_+^{μ} and l_-^{μ} point towards increasing and decreasing y , respectively. Hence, we adopt the usual convention and refer to l_+^{μ} (l_-^{μ}) and the corresponding null geodesics as outgoing (ingoing) although increasing (decreasing) y does not necessarily imply increasing (decreasing) of the radial coordinate r . As we move along a geodesic the changes of the coordinates τ and y are subject to the condition $ds = 0$ of radial null geodesics, i.e.,

$$d\tau = \pm \frac{\alpha}{\beta} dy \quad (43)$$

along the geodesic. Here the signs determine whether y is increasing or decreasing as we move along the geodesic. For example, for future directed null geodesics, it follows from (41) and (43) that an outgoing geodesic is directed along increasing y , i.e., y increases with λ_+ , whereas an ingoing geodesic is directed along decreasing y , i.e., y decreases with λ_- .

The key roles in the study of trapped surfaces are played by the expansion parameters ε_+ and ε_- ,

$$\varepsilon_{\pm} = \nabla_{\mu} l_{\pm}^{\mu} \quad (44)$$

of outgoing and ingoing null geodesics, respectively. Particularly important are the values of ε_+ and ε_- and their Lie derivatives,

$$\frac{d\varepsilon_+}{d\lambda_-} \equiv l_-^{\mu} \partial_{\mu} \varepsilon_+; \quad \frac{d\varepsilon_-}{d\lambda_+} \equiv l_+^{\mu} \partial_{\mu} \varepsilon_- \quad (45)$$

in the neighborhood of a marginally trapped surface. As we shall shortly demonstrate, the relevant marginally trapped surface in the expanding chiral fluid is future inner marginally trapped. According to our convention described in the Appendix A, a two-dimensional surface H is said to be *future inner marginally trapped* if the future directed null expansions on H satisfy the conditions: $\varepsilon_+|_H = 0$, $l_-^{\mu} \partial_{\mu} \varepsilon_+|_H > 0$ and $\varepsilon_-|_H < 0$. The future inner marginally trapped surface is the *inner* boundary of a future trapped region consisting of trapped surfaces with negative ingoing and outgoing null expansions. From now on we refer to this surface as the *apparent horizon*.

From (39) and (40) we find

$$\varepsilon_{\pm} = \frac{2}{\alpha^2} \left(\frac{\dot{\alpha}}{\beta} \pm \frac{1}{\tanh y} \right) \quad (46)$$

for future directed and

$$\varepsilon_{\pm} = \frac{2}{\alpha^2} \left(-\frac{\dot{\alpha}}{\beta} \pm \frac{1}{\tanh y} \right) \quad (47)$$

for past directed radial null geodesics, where the overdot denotes a partial derivative with respect to τ . The respective Lie derivatives are given by

$$\frac{d\varepsilon_{\pm}}{d\lambda_{\mp}} \equiv l_{\mp}^{\mu} \partial_{\mu} \varepsilon_{\pm} = \frac{2}{\alpha^2 \beta^2} \left[\frac{\ddot{\alpha}}{\alpha} - \frac{\dot{\alpha}\dot{\beta}}{\alpha\beta} - \left(1 - \frac{1}{\tanh^2 y} \right) \frac{\beta^2}{\alpha^2} \right] - \frac{2\dot{\alpha}}{\alpha^2 \beta} \varepsilon_{\pm}, \quad (48)$$

for future directed and

$$\frac{d\varepsilon_{\pm}}{d\lambda_{\mp}} \equiv l_{\mp}^{\mu} \partial_{\mu} \varepsilon_{\pm} = \frac{2}{\alpha^2 \beta^2} \left[\frac{\ddot{\alpha}}{\alpha} - \frac{\dot{\alpha} \dot{\beta}}{\alpha \beta} + \left(1 - \frac{1}{\tanh^2 y} \right) \frac{\beta^2}{\alpha^2} \right] + \frac{2\dot{\alpha}}{\alpha^2 \beta} \varepsilon_{\pm}, \quad (49)$$

for past directed radial null geodesics.

For a spherically symmetric spacetime, the condition that one of the null expansions vanishes on the apparent horizon H is equivalent to the condition that the vector n_{μ} , normal to the surface of spherical symmetry, is null on H . In other words, the condition

$$\nabla_{\mu} l^{\mu}|_H = 0, \quad (50)$$

where l^{μ} denotes either l_{+}^{μ} or l_{-}^{μ} , is equivalent to the condition

$$G^{\mu\nu} n_{\mu} n_{\nu}|_H = 0. \quad (51)$$

This may be seen as follows. For the metric (36) the normal n_{μ} is given by

$$n_{\mu} = \partial_{\mu}(\alpha \sinh y). \quad (52)$$

The expansion ε_{+} (or ε_{-}) defined in (44) may be written as

$$\nabla_{\mu} l^{\mu} = \frac{1}{\sqrt{-G}} \partial_{\mu}(\sqrt{-G} l^{\mu}) = \frac{1}{\sqrt{-h}} \partial_{\mu}(\sqrt{-h} l^{\mu}) + \frac{2}{\alpha \sinh y} l^{\mu} n_{\mu} \quad (53)$$

where h denotes the determinant of the metric

$$h_{\alpha\beta} = \begin{pmatrix} \beta^2 & 0 \\ 0 & -\alpha^2 \end{pmatrix}, \quad (54)$$

of the two-dimensional space normal to the surface of spherical symmetry. It may be shown that the first term on the right-hand side of (53) vanishes identically by the geodesic equation. Hence, the expansion $\nabla_{\mu} l^{\mu}$ vanishes on H if and only if

$$l^{\beta} n_{\beta}|_H = 0. \quad (55)$$

Suppose one of the expansions vanishes on H , i.e., Eq. (55) holds for either l_{+}^{μ} or l_{-}^{μ} . Since l^{μ} is null and both l^{μ} and n^{μ} are normal to H and hence tangent to the two-dimensional space (τ, y) with the metric (54), Eq. (55) implies $h_{\alpha\beta} n^{\alpha} n^{\beta}|_H = 0$. Hence, $\nabla_{\mu} l^{\mu}|_H = 0$ implies $G^{\mu\nu} n_{\mu} n_{\nu}|_H = 0$.

To prove the reverse it is sufficient to show that $l_{+}^{\beta} n_{\beta} \neq 0$ and $l_{-}^{\beta} n_{\beta} \neq 0$ implies $h_{\alpha\beta} n^{\alpha} n^{\beta} \neq 0$, which may be easily shown for a general two-dimensional metric in diagonal gauge. Then, the following statement holds: the vanishing of $h_{\alpha\beta} n^{\alpha} n^{\beta}$ on H implies either $l_{+}^{\beta} n_{\beta}|_H = 0$ or $l_{-}^{\beta} n_{\beta}|_H = 0$. This together with (53), implies either $\varepsilon_{+}|_H = 0$ or $\varepsilon_{-}|_H = 0$.

Either from (50) or (51) one finds the condition for the apparent horizon

$$\frac{\dot{\alpha}}{\beta} \pm \frac{1}{\tanh y} = 0 \quad (56)$$

3.2 Analog horizons

Next we derive the analog metric and define the analog Hubble and the apparent horizons. Equation (12) may be written in the form [14, 33, 34]

$$\frac{1}{\sqrt{-G}} \partial_\mu (\sqrt{-G} G^{\mu\nu}) \partial_\nu \boldsymbol{\pi} + \frac{c_\pi^2}{a} V(\sigma, \boldsymbol{\pi}) \boldsymbol{\pi} = 0, \quad (57)$$

with the analog metric tensor, its inverse, and its determinant given by

$$G_{\mu\nu} = \frac{a}{c_\pi} [g_{\mu\nu} - (1 - c_\pi^2) u_\mu u_\nu], \quad (58)$$

$$G^{\mu\nu} = \frac{c_\pi}{a} \left[g^{\mu\nu} - \left(1 - \frac{1}{c_\pi^2}\right) u^\mu u^\nu \right], \quad (59)$$

$$G = \frac{a^4}{c_\pi^2} g. \quad (60)$$

Hence, the pion field propagates in a (3+1)-dimensional effective geometry described by the metric $G_{\mu\nu}$.

In the comoving coordinate frame defined by the coordinate transformation (26) the velocity is $u^\mu = (1, 0, 0, 0)$ and, as a consequence, the analog metric (58) is diagonal

$$G_{\mu\nu} = \frac{a}{c_\pi} \begin{pmatrix} c_\pi^2 & & & \\ & -\tau^2 & & \\ & & -\tau^2 \sinh^2 y & \\ & & & -\tau^2 \sinh^2 y \sin^2 \vartheta \end{pmatrix}. \quad (61)$$

Here, the parameters a and c_π are functions of the temperature T , which in turn is a function of τ . In the following we assume that these functions are positive. The metric (61) is precisely of the form (36) with

$$\beta(\tau) = \sqrt{ac_\pi}; \quad \alpha(\tau) = \tau \sqrt{\frac{a}{c_\pi}}. \quad (62)$$

The physical range of τ is fixed by Eq. (34) since the available temperature ranges are between $T = 0$ and $T = T_c$. Hence, the proper time range is $\tau_c \leq \tau < \infty$, where the critical value τ_c is related to the critical temperature as $\tau_c/\tau_0 = T_0/T_c$. The metric is singular at $\tau = \tau_c$.

In Fig. 3 we plot the expansions ε_+ and ε_- of outgoing and ingoing radial null geodesics, respectively, as functions of r for an arbitrarily chosen fixed time $t = 6t_0$ and, similarly, as functions of y for a fixed $\tau = 5.77\tau_0$. In the lower two panels we plot the derivative of the outgoing null expansion ε_+ along the ingoing null geodesic. The outgoing null expansion decreases with increasing r from positive to negative values and vanishes at the point $r = r_H$, whereas the ingoing null expansion remains negative. At this point the derivative of ε_+ with respect to λ_- is positive. According to the standard convention described in Appendix A the region $\{r > r_H, t = 6\tau_0\}$ is future trapped and the location r_H marks its inner boundary. Thus, the sphere at r_H is future inner marginally trapped.

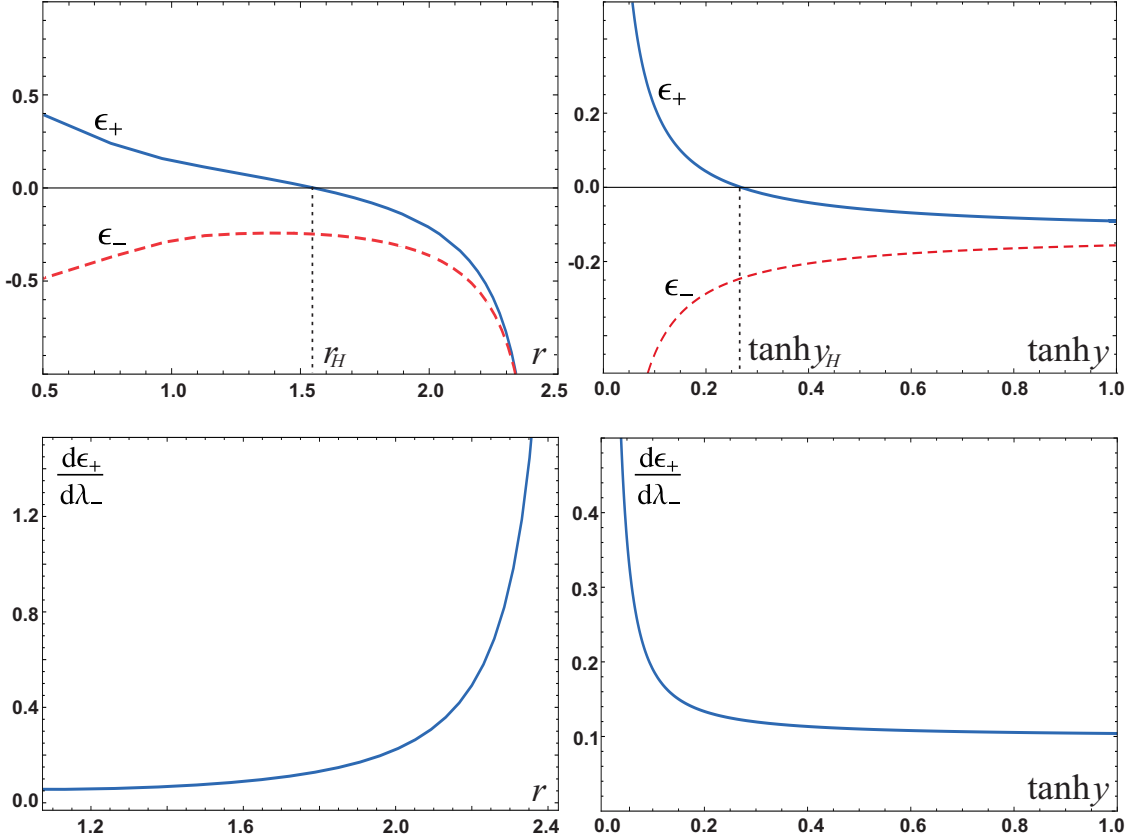


Figure 3: Null expansions ε_+ and ε_- as functions of r (top left panel) and y (top right panel) for fixed $t = 6\tau_0$ and fixed $\tau = 5.77\tau_0$, respectively. Similarly, the bottom panels depict the derivative of ε_+ as functions of r and y for fixed t and τ , respectively.

Spacetime diagram corresponding to the metric (61) is presented in Fig. 4, showing future directed radial null geodesics. The origin in the plots in both panels corresponds to the critical value τ_c at which c_π vanishes. Numerically, with the chosen $T_0 = 1$ GeV we have $\tau_c/\tau_0 = 5.47$. The geodesic lines are constructed using

$$y = \pm \int_{\tau_c}^{\tau} d\tau' c_\pi(\tau')/\tau' + \text{const} \quad (63)$$

which follows from (43) with (62). As mentioned in Sec. 3.1, increasing (decreasing) y does not necessarily imply increasing (decreasing) of the radial coordinate r . With the help of the coordinate transformation (26) the shift dy along a geodesic may be expressed in terms of dr

$$dy = \frac{c_\pi}{(c_\pi \pm v)\tau \cosh y} dr. \quad (64)$$

where we have used (25) and (62). We note that if $v < c_\pi$, increasing (decreasing) y corresponds to increasing (decreasing) r for both signs, whereas if $v > c_\pi$ increasing y corresponds to increasing r for an outgoing and decreasing r for an ingoing geodesic.

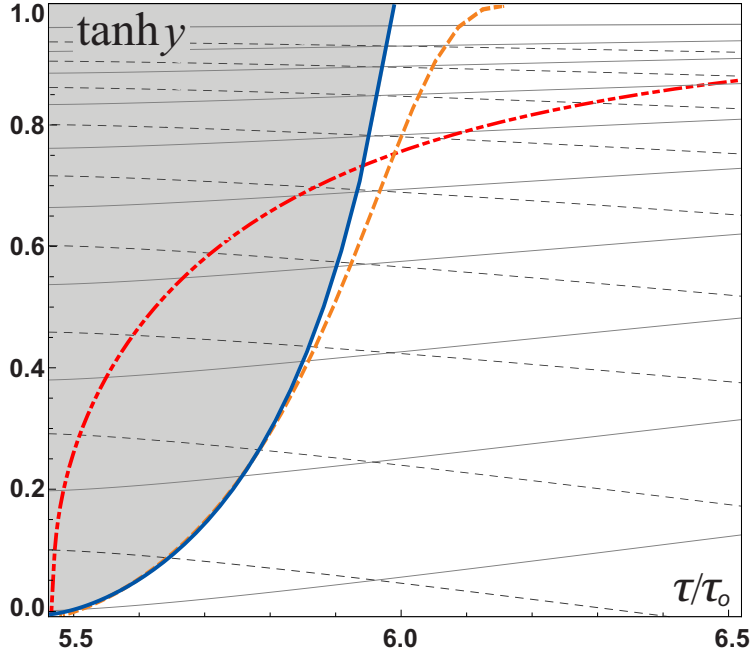


Figure 4: Spacetime diagram of outgoing (full line) and ingoing (dashed line) radial null geodesics in (τ, y) coordinates. The shaded area represents the evolution of the trapped region. The trapping horizon is represented by the full bold line with the endpoint at $\tau = \tau_{\max} = 6.0182\tau_0$. The dashed and dash-dotted bold lines represent the evolution of the analog and naive Hubble horizons, respectively.

Using (63) we introduce null coordinates

$$w = \frac{1}{2} \left(y + \int_{\tau_c}^{\tau} d\tau' \beta(\tau') / \alpha(\tau') \right); \quad u = \frac{1}{2} \left(-y + \int_{\tau_c}^{\tau} d\tau' \beta(\tau') / \alpha(\tau') \right), \quad (65)$$

ranging in the intervals $[0, +\infty)$ and $(-\infty, +\infty)$, respectively, with a condition $0 \leq w \pm u < \infty$. In these coordinates the metric (35) becomes

$$ds^2 = \alpha^2 \left(4dudw - \sinh^2(w - u) d\Omega^2 \right). \quad (66)$$

The singularity at $\tau = \tau_c$ is mapped onto the entire $u + w = 0$ line. Next, we compactify the spacetime using the coordinate transformation

$$W = \tanh w; \quad U = \tanh u. \quad (67)$$

The coordinates W and U range in the intervals $[0, 1]$ and $[-1, 1]$, respectively, with a condition $0 \leq W \pm U \leq 2$. Furthermore, the rotation

$$T = \frac{1}{\sqrt{2}}(W + U); \quad R = \frac{1}{\sqrt{2}}(W - U), \quad (68)$$

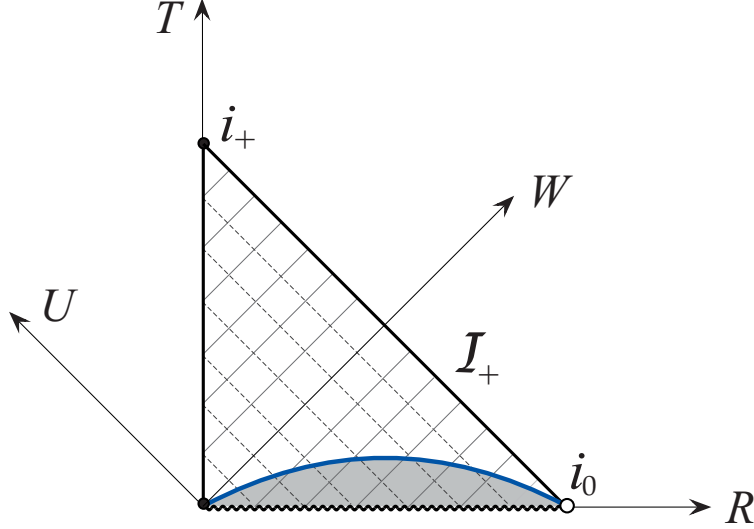


Figure 5: Conformal diagram for the analog spacetime described by the metric (61). The lines parallel to the W and U axes, are future directed outgoing and ingoing null geodesics, respectively. The singularity at $\tau = \tau_c$ is represented by the wavy line and the apparent horizon by the full line. The shaded area in between represents the evolution of the trapped region. The spacelike and future timelike infinities are denoted by i_0 and i_+ , respectively. The future null infinity \mathcal{I}_+ is represented by the line $T + R = \sqrt{2}$.

brings the metric to a conformally flat form

$$ds^2 = \frac{2\alpha^2}{(1-U^2)(1-W^2)} [dT^2 - dR^2 - R^2 d\Omega^2], \quad (69)$$

where both coordinates R and T range in the interval $[0, \sqrt{2}]$ with a condition $R + T \leq \sqrt{2}$. The conformal diagram representing our analog spacetime is depicted in Fig. 5. The singularity at $\tau = \tau_c$ is mapped onto the segment $[0, \sqrt{2}]$ on the horizontal axis.

The coordinate transformation

$$t' = \int \beta d\tau \quad (70)$$

brings the metric (61) to the standard form of an open $k = -1$ FRW spacetime metric with the cosmological time t' . The time coordinate t' is related to the original time t via τ and the transformation (26). The analog cosmological scale is $a(t') = \alpha(\tau(t'))/r_0$, where the constant r_0 is related to the spatial Gaussian curvature $K = -1/r_0^2$. The proper distance is $d_p = \alpha y$ and the analog Hubble constant is

$$\mathcal{H} = \frac{\dot{\alpha}}{\alpha\beta}, \quad (71)$$

where the overdot denotes a partial derivative with respect to τ . Then, we define the *analog Hubble horizon* as a two-dimensional spherical surface at which the magnitude of the analog

recession velocity

$$v_{\text{rec}} = \mathcal{H}d_p = y \frac{\dot{\alpha}}{\beta} \quad (72)$$

equals the velocity of light. Hence, the condition

$$y = \frac{\beta}{|\dot{\alpha}|} \quad (73)$$

defines the location of the analog Hubble horizon. Note that the radial fluid velocity v in (25) and the analog recession velocity (72) are quite distinct quantities – in an expanding fluid v is always positive and less than the velocity of light $c = 1$, whereas v_{rec} may be positive or negative depending on the sign of $\dot{\alpha}$ and its magnitude may be arbitrarily large.

A two-dimensional spherical surface on which the radial velocity v equals the velocity of pions c_π defines another horizon, which we refer to as the *naive Hubble horizon*. This horizon is obviously distinct from the analog Hubble horizon defined above. The evolution of the naive and the analog Hubble horizons with τ are depicted in Fig. 4.

Next we introduce the concept of an analog marginally trapped surface or *analog apparent horizon* following closely the general considerations of Sec. 3.1 and the Appendix A. The formation of an analog apparent horizon in an expanding hadronic fluid is similar to the formation of a black hole in a gravitational collapse although the role of an outer trapped surface is exchanged with that of an inner trapped surface. Unlike a black hole in general relativity, the formation of which is indicated by the existence of an *outer* marginally trapped surface, the formation of an analog black (or white) hole in an expanding fluid is indicated by the existence of a future or past *inner* marginally trapped surface.

Equation (56) with (62) defines a hypersurface which we refer to as the *analog trapping horizon*. Any solution to Eq. (56), e.g., in terms of r for fixed t , gives the location of the analog apparent horizon r_H . For example, the radius $r_H = 1.53\tau_0$ computed using (56) for fixed $t = 6t_0$ is the point of vanishing outgoing null expansion which marks the location of the apparent horizon in the top left panel of Fig. 3. From (46) it follows that the region of spacetime for which

$$\tanh y \geq |\beta/\dot{\alpha}| \quad (74)$$

is trapped. It is future trapped if $\dot{\alpha} < 0$ and past trapped if $\dot{\alpha} > 0$. The condition (74) can be met only if $|\beta/\dot{\alpha}| \leq 1$, which holds for τ between τ_c and τ_{max} . At $\tau = \tau_{\text{max}}$ we have $|\beta/\dot{\alpha}| = 1$, so the endpoint of the trapping horizon in Fig. 4 is at $\tau = \tau_{\text{max}}$, $\tanh y = 1$.

We find that $\dot{\alpha}$ is negative for τ in the entire range $\tau_c \leq \tau \leq \tau_{\text{max}}$ and, according to (71), the analog Hubble constant is always negative. Hence, our analog cosmological model is a contracting FRW spacetime with a negative spatial curvature. The shaded area left of the bold line in Fig. 4 represents the time evolution of the future trapped region. Note that the analog Hubble horizon is always behind the apparent horizon whereas the naive Hubble horizon may be located ahead of or behind the apparent horizon depending on the magnitude of $\dot{\alpha}$. The naive Hubble and apparent horizons coincide if a and c_π are τ independent constants.

The apparent horizon is generally not a Killing horizon and normally does not coincide with the event horizon (one exception is de Sitter spacetime). Moreover, the apparent horizon exists in all FRW universes [35], whereas the event horizon does not exist in eternally

expanding FRW universes with the equation of state $w > -1/3$ (see, e.g., [36]). For the metric (61), the event horizon is defined by

$$y = \int_{\tau}^{\infty} d\tau' \frac{c_{\pi}(\tau')}{\tau'}. \quad (75)$$

In our chiral fluid model the integral on the right-hand side diverges at the upper limit because $c_{\pi} \rightarrow 1$ as $\tau \rightarrow \infty$ and hence, the analog event horizon does not exist. In contrast, as we have demonstrated, the analog apparent horizon does exist.

3.3 Analog Hawking effect

One immediate effect related to the apparent horizon is the Hawking radiation. Unfortunately, in a nonstationary spacetime, the surface gravity associated to the apparent horizon is not uniquely defined [37]. Several ideas have been put forward how to generalize the definition of surface gravity for the case when the apparent horizon does not coincide with the event horizon [38, 39, 40, 41]. In this paper we use the prescription of [41] which we have adapted to analog gravity in our previous paper [16]. This prescription involves the so-called Kodama vector K^{μ} [42] which generalizes the concept of the time translation Killing vector to nonstationary spacetimes. The analog surface gravity κ is defined by

$$\kappa = \frac{1}{2} \frac{1}{\sqrt{-h}} \partial_{\alpha} (\sqrt{-h} h^{\alpha\beta} k n_{\beta}), \quad (76)$$

where the quantities on the right-hand side should be evaluated on the trapping horizon. The metric $h_{\alpha\beta}$ of the two-dimensional space normal to the surface of spherical symmetry and the vector n_{α} normal to that surface are given by (54) and (52), respectively.

The definition (76) differs from the original expression for the dynamical surface gravity [41, 43] by a normalization factor k which we have introduced in order to meet the requirement that K^{μ} should coincide with the time translation Killing vector ξ^{μ} for a stationary geometry. For the metric (61) with (62) we have found [16]

$$k = \beta \left(\cosh^2 y - \sinh^2 y \frac{\tau \dot{\alpha}}{\alpha} \right). \quad (77)$$

Then, the definition (76) yields

$$\kappa = \frac{v}{2\beta\gamma(\alpha - \tau\dot{\alpha}v^2)^2} \left[\alpha(\dot{\alpha}^2 + \alpha\ddot{\alpha} - \beta^2) + 2\beta^2(\tau\dot{\alpha} - \alpha)v + (\alpha\dot{\alpha}^2 - 2\tau\dot{\alpha}^3 + \beta^2\tau\dot{\alpha})v^2 \right] \quad (78)$$

evaluated on the trapping horizon. The above expression may be somewhat simplified by making use of the horizon condition (56). We find

$$\kappa = \frac{c_{\pi}}{2\tau} \frac{1 + 2c_{\pi}v(1-v) - (2+c_{\pi})v^3}{\gamma v(1+c_{\pi}v)^2} + \frac{\ddot{\alpha}}{2\beta} \frac{v}{\gamma(1+c_{\pi}v)^2} \quad (79)$$

evaluated on the trapping horizon.

It is worthwhile analyze the limiting case of (78) when the quantities a and c_{π} are constants. Then $\dot{\alpha} = \alpha/\tau$, $\ddot{\alpha} = 0$, and the apparent horizon is fixed by the condition $v = c_{\pi}$.

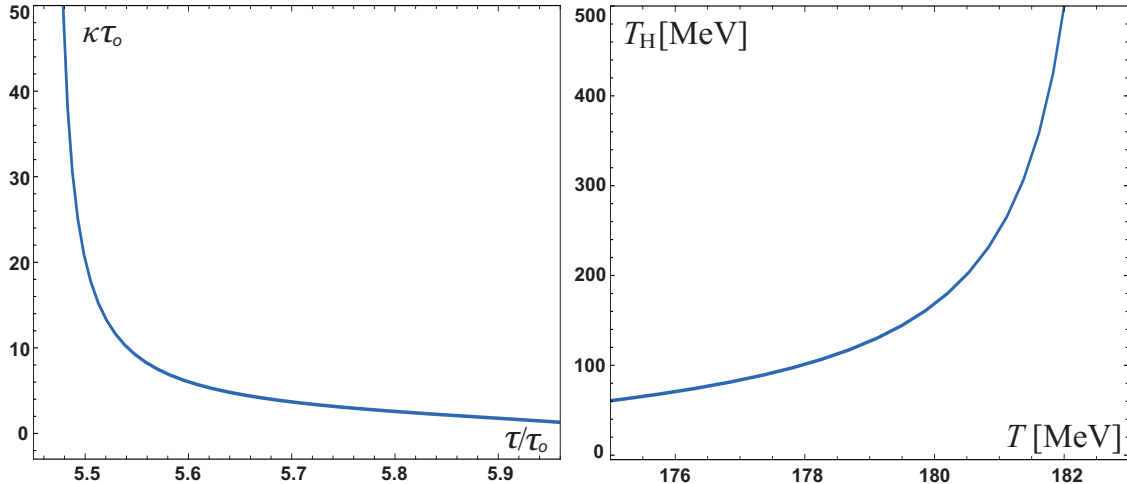


Figure 6: Analog surface gravity as a function of the proper time τ (left panel) and the corresponding Hawking temperature as a function of the fluid temperature T (right panel).

At any chosen time $t = \tau(1 - c_\pi^2)^{-1/2}$ the horizon is located at $r_H = c_\pi t$ and the expression for κ reduces to

$$\kappa = \frac{1}{2t} = \frac{\sqrt{1 - c_\pi^2}}{2\tau} \quad (80)$$

Hence, the analog surface gravity is finite for any physical value of c_π and is maximal when $c_\pi = 0$. However, with $c_\pi = 0$ the horizon degenerates to a point located at the origin $r = 0$.

In the left panel of Fig. 6 we plot κ as a function of τ as given by (79). The corresponding temperature defined as

$$T_H = \frac{\kappa}{2\pi} \quad (81)$$

represents the analog Hawking temperature of thermal pions emitted at the apparent horizon as measured by an observer near infinity. Since the background geometry is flat, this temperature equals the locally measured Hawking temperature at the horizon. Thus, Eq. (81) with (78) corresponds to the flat spacetime Unruh effect.

As we move along the trapping horizon the radius of the apparent horizon increases and the Hawking temperature decreases rapidly with τ . Hence, there is a correlation between T_H and the local fluid temperature T which is related to τ by (34). In the right panel of Fig. 6 we show the Hawking temperature T_H as a function of the fluid temperature T at the apparent horizon.

In our previous paper [16] we showed that the surface gravity diverges as

$$\kappa = (\eta + 1/2)(\tau - \tau_c)^{-1} \quad (82)$$

at the singular point, where η is a constant related to the scaling of the quantity $\sqrt{a/c_\pi}$

$$\sqrt{\frac{a}{c_\pi}} \propto (T_c - T)^{-\eta} \quad (83)$$

in the neighborhood of the critical point. The constant η may be roughly estimated as follows. The estimate of the function $\Sigma(q)$ defined in (19) in the neighborhood of $q^\mu = 0$ for small σ yields [24]

$$\Sigma(0, \mathbf{q}^2) \sim \frac{T}{\sigma} \mathbf{q}^2; \quad \Sigma(q_0, 0) \sim \frac{T^2}{\sigma^2} q_0^2 \quad (84)$$

By comparing this with (18) we deduce the behavior of the quantities a and b for small σ

$$a \sim \frac{T}{\sigma}; \quad a + b \sim \frac{T^2}{\sigma^2}. \quad (85)$$

Then, from (15) the pion velocity goes to zero approximately as $c_\pi \propto \sigma^{1/2}$ whereas the ratio a/c_π diverges as $a/c_\pi \propto \sigma^{-3/2}$. From Eq. (8) we find $\sigma \propto (T_c - T)^{1/2}$ near the critical point which yields $\eta = 3/8$.

Numerically, by fitting $\sqrt{a/c_\pi}$ in the close neighborhood of T_c to the function (83) with the critical temperature $T_c = 182.822$ MeV obtained numerically from (8), we find $\eta = 0.253$. A more refined analysis based on scaling and universality arguments of Son and Stephanov [23] yields $\eta = 0.1975$ [16].

4 Summary and discussion

We have demonstrated that, owing to the analog gravity effects in high energy collisions, a close analogy may be drawn between the evolution of a hadronic fluid and the spacetime expansion. Using the formalism of relativistic acoustic geometry we have analyzed the expanding chiral fluid in the regime of broken chiral symmetry. The expansion which takes place after the collision is modeled by spherically symmetric Bjorken type expansion. The propagation of massless pions in the chiral fluid provides a geometric analog of expanding spacetime equivalent to an open ($k = -1$) FRW cosmology. The geometry depends on the parameters a and b of the effective Lagrangian defined in Sec. 2. The elements of the analog metric tensor are functions of the spacetime coordinates via the temperature dependence of a and the pion velocity c_π . The pions propagate slower than light with a velocity close to zero in the neighborhood of the critical point of the chiral phase transition.

A trapped region forms for radial velocities of the fluid beyond the value defined by Eq. (56). This value defines a hypersurface shown in Fig. 4 which we refer to as the analog trapping horizon, at which the outgoing radial null expansion vanishes. Our trapping horizon is foliated by future inner marginally trapped surfaces and is equivalent to the trapping horizon in contracting FRW spacetime, i.e., in dynamical spacetime with a negative Hubble constant. The shaded area in Fig. 4 represents the time evolution of the future trapped region, with the future inner marginally trapped surface (or the future apparent horizons) as its inner boundary. This marginally trapped surface may be regarded as an ‘‘outer’’ white hole: the ingoing pions (future directed ingoing null geodesics) freely cross the apparent horizon whereas the outgoing cannot penetrate the apparent horizon. This is opposite to an expanding FRW universe where the inner marginally trapped surface acts as a black hole: the future directed ingoing null geodesics cannot escape the apparent horizon whereas the outgoing null geodesics freely cross the apparent horizon.

We have studied the Hawking effect associated with the analog apparent horizon using the Kodama-Hayward definition of surface gravity adapted to the analog gravity geometry. The Hawking temperature correlates with the local temperature of the fluid at the apparent horizon and diverges at the critical point. In contrast to the usual general relativistic Hawking effect, where the Hawking temperature is tiny compared with the temperature of the background, the analog horizon temperature is of the order or even larger than the local temperature of the fluid.

The most important outcome of our analysis relevant for particle physics phenomenology is thermal radiation of pions due to the analog Hawking effect. In that regard, it is tempting to speculate about possible signals for the analog Hawking effect in high energy collisions. In principle, one could measure the temperature by fitting the pion spectrum to the thermal Planck distribution. However, one additional signal should be invented in order to unambiguously distinguish between the thermal pions produced above the critical temperature from those emitted as an analog Hawking radiation from the apparent horizon below the critical temperature.

The analog Hawking radiation of pions should not be confused with the Hawking-Unruh radiation of hadrons of Castorina *et al.* [44]. The latter is a usual Unruh effect due to the acceleration of quark-antiquark pairs produced in particle collisions, whereas the former is an analog thermal radiation due to effective geometry of the chiral fluid.

A spherically symmetric Bjorken expansion model considered here may be phenomenologically viable as a model of hadron production in e^+e^- , but it is certainly not the best model for description of high energy heavy ion collisions. It would be desirable to apply our formalism to a more realistic hydrodynamic model that involves a transverse expansion superimposed on a longitudinal boost invariant expansion. In this case the calculations become rather involved, as the formalism for general nonspherical spacetimes is not yet fully developed. This work is in progress.

In conclusion, we believe that the study of analog gravity in high energy collision may in general improve our understanding of both particle physics phenomenology and dynamical general relativistic systems.

Acknowledgments

This work was supported by the Ministry of Science, Education and Sport of the Republic of Croatia under Contract No. 098-0982930-2864 and partially supported by the ICTP-SEENET-MTP Grant No. PRJ-09 “Strings and Cosmology“ in the frame of the SEENET-MTP Network.

A Trapped surfaces in general relativity

Following Hayward, [40] we summarize here the relevant definitions related to trapped surfaces.

1. *Trapped surface*: Let Σ denote a spacelike hypersurface, e.g., a hypersurface defined by $t = \text{const}$. A two-dimensional surface $S \subset \Sigma$ with spherical topology is called a *trapped*

surface on Σ if the families of ingoing and outgoing null geodesics normal to the surface are both converging or both diverging. More precisely, the null expansions $\varepsilon_+ = l_{+;\mu}^\mu$ and $\varepsilon_- = l_{-;\mu}^\mu$ on a trapped surface S should satisfy $\varepsilon_+\varepsilon_- > 0$. One distinguishes between a *past trapped surface* for which both ε_+ and ε_- are positive, and a *future trapped surface* for which both ε_+ and ε_- are negative.

2. *Trapped region*: A set of future trapped surfaces (or closed trapped surfaces [35, 45]) on Σ is referred to as a *future trapped region*. Similarly, a set of past trapped surfaces on Σ is called a *past trapped region*.
3. *Marginally trapped surface*: A two-dimensional surface H is said to be *marginally trapped* if one of the null expansions vanishes on H , i.e., if either $\varepsilon_+|_H = 0$ or $\varepsilon_-|_H = 0$. A marginally trapped surface is also referred to as an *apparent horizon* although, strictly speaking, the original definition of Ellis and Hawking [45] involves in addition the assumption of asymptotic flatness.
4. *Outer marginally trapped surface*: A surface H is said to be future (past) outer marginally trapped if on H the future (past) directed outgoing null expansion vanishes, its derivative along the ingoing null geodesic is negative, and the ingoing null expansion is negative, i.e., if $\varepsilon_+|_H = 0$, $l_-^\mu \partial_\mu \varepsilon_+|_H < 0$, and $\varepsilon_-|_H < 0$. Equivalently, the future (past) outer marginally trapped surface may be defined as the surface on which the past (future) directed ingoing null expansion vanishes, its derivative along the outgoing null geodesic is negative, and the outgoing null expansion is positive, i.e., if $\varepsilon_-|_H = 0$, $l_+^\mu \partial_\mu \varepsilon_-|_H < 0$, and $\varepsilon_+|_H > 0$.
5. *Inner marginally trapped surface*: A surface H is said to be future (past) inner marginally trapped if on H the future (past) directed outgoing null expansion vanishes, its derivative along the ingoing null geodesic is positive, and the ingoing null expansion is negative, i.e., if $\varepsilon_+|_H = 0$, $l_-^\mu \partial_\mu \varepsilon_+|_H > 0$, and $\varepsilon_-|_H < 0$. Equivalently, the future (past) inner marginally trapped surface may be defined as the surface on which the past (future) directed ingoing null expansion vanishes, its derivative along the outgoing null geodesic is positive, and the outgoing null expansion is positive, i.e., ($\varepsilon_-|_H = 0$, $l_+^\mu \partial_\mu \varepsilon_-|_H > 0$, and $\varepsilon_+|_H > 0$).
6. *Trapping horizon*: A hypersurface foliated by inner or outer marginally trapped surfaces is referred to as an inner or outer *trapping horizon*, respectively.

According to this classification we distinguish four physically relevant classes:

- i. A *future outer marginally trapped surface* is the outer boundary of a future trapped region and is typical of a black hole.
- ii. A *past outer marginally trapped surface* is the outer boundary of a past trapped region and is typical of a white hole.
- iii. A *future inner marginally trapped surface* is the inner boundary of a future trapped region and represents an "outer" white hole. This situation is physically relevant in the cosmological context for a shrinking universe, i.e., for an FRW spacetime with $\dot{a} < 0$.

- iv. *A past inner marginally trapped surface* is the inner boundary of a past trapped region and represents an “outer” black hole. This situation is physically relevant in the context of an expanding FRW universe [35, 46].

References

- [1] U. W. Heinz, C. Shen, and H. Song, in the AIP Conference Proceedings PANIC11 MIT, 24-29 July 2011 (to be published).
- [2] M. Floris (ALICE collaboration), J. Phys. G **38**, 124025 (2011); arXiv:1108.3257.
- [3] CERN Courier, **52**, January/February 2012, p. 8
- [4] C. Shen, U. Heinz, P. Huovinen, and H. Song, Phys. Rev. C **84**, 044903 (2011).
- [5] A. Dumitru, Phys. Lett. B **463**, 138 (1999); P. F. Kolb, U. W. Heinz, P. Huovinen, K. J. Eskola, and K. Tuominen, Nucl. Phys. A **696**, 197 (2001).
- [6] J. D. Bjorken, Phys. Rev. D **27**, 140 (1983).
- [7] M. Tuts, CNN, 9 November 2010.
- [8] BBC News, 8 November 2010.
- [9] D. Evans, The Telegraph, 8 November 2010.
- [10] C. Barcelo, S. Liberati, and M. Visser, Living Rev. Rel. **14**, 3 (2011); gr-qc/0505065.
- [11] M. Visser, Class. Quant. Grav. **15**, 1765–1791 (1998).
- [12] T. G. Philbin, C. Kuklewicz, S. Robertson, S. Hill, F. Konig, and U. Leonhardt, Science **319**, 1367 (2008).
- [13] T.A. Jacobson and G.E. Volovik, Phys. Rev. D **58**, 064021 (1998).
- [14] V. Moncrief, Astrophys. J. **235**, 1038-46 (1980).
- [15] H. Abraham, N. Bilić and T. K. Das, Class. Quant. Grav. **23**, 2371 (2006); gr-qc/0509057; T. K. Das, N. Bilić and S. Dasgupta, JCAP **0706**, 009 (2007); astro-ph/0604477.
- [16] N. Bilić and D. Tolić, Phys. Lett. B **718**, 1 (2012), arXiv:1207.2869,
- [17] M.A. Shifman, Ann. Rev. Nucl. Part. Sci. **33**, 199 (1983).
- [18] J. W. Harris and B. Müller, Ann. Rev. Nucl. Part. Sci. **46**, 71 (1996).
- [19] N. Bilić, J. Cleymans, and M. D. Scadron, Int. J. Mod. Phys. **A10**, 1169 (1995).
- [20] N. Bilić and H. Nikolić, Eur. Phys. J. C **6**, 515 (1999).

- [21] M. Gell-Mann and M. Lévy, *Nuovo Cimento* **16**, 705 (1960).
- [22] R. D. Pisarski and M. Tytgat, *Phys. Rev. D* **54**, R2989 (1996).
- [23] D. T. Son and M. A. Stephanov, *Phys. Rev. Lett.* **88**, 202302 (2002).
- [24] D. T. Son and M. A. Stephanov, *Phys. Rev. D* **66**, 076011 (2002).
- [25] M. A. Lampert, J. F. Dawson and F. Cooper, *Phys. Rev. D* **54**, 2213 (1996); G. Amelino-Camelia, J. D. Bjorken and S. E. Larsson, *Phys. Rev. D* **56**, 6942 (1997); M. A. Lampert and C. Molina-Paris, *Phys. Rev. D* **57**, 83 (1998); A. Krzywicki and J. Serreau, *Phys. Lett. B* **448**, 257 (1999).
- [26] N. Bilić and H. Nikolić, *Phys. Rev. D* **68**, 085008 (2003); hep-ph/0301275.
- [27] H. Meyer-Ortmanns and B.-J. Schaefer, *Phys. Rev. D* **53**, 6586 (1996).
- [28] D. Röder, J. Ruppert, and D. H. Rischke, *Phys. Rev. D* **68**, 016003 (2003).
- [29] R. D. Pisarski and F. Wilczek, *Phys. Rev. D* **29**, 338 (1984).
- [30] J. Baacke and S. Michalski, *Phys. Rev. D* **67**, 085006 (2003).
- [31] L.D. Landau and E.M. Lifshitz, *Statistical Physics*, (Pergamon, Oxford, 1993) p. 187.
- [32] P. F. Kolb, J. Sollfrank, and U. W. Heinz, *Phys. Rev. C* **62**, 054909 (2000). V. N. Russkikh and Y. .B. Ivanov, *Phys. Rev. C* **76**, 054907 (2007).
- [33] N. Bilić, *Class. Quantum Grav.* **16**, 3953 (1999).
- [34] M. Visser and C. Molina-Paris, *New J. Phys.* **12**, 095014 (2010).
- [35] G. F. R. Ellis, *Gen. Rel. Grav.* **35**, 1309 (2003).
- [36] T. M. Davis and C. H. Lineweaver, *PASA*, 21, 97-109 (2004); astro-ph/0310808.
- [37] A. B. Nielsen and J. H. Yoon, *Class. Quant. Grav.* **25**, 085010 (2008).
- [38] G. Fodor, K. Nakamura, Y. Oshiro, and A. Tomimatsu, *Phys. Rev. D* **54**, 3882 (1996).
- [39] S. Mukohyama and S. A. Hayward, *Class. Quant. Grav.* **17**, 2153 (2000); I. Booth and S. Fairhurst, *Phys. Rev. Lett.* **92**, 011102 (2004).
- [40] S. A. Hayward, *Phys. Rev. D* **49**, 6467 (1994).
- [41] S. A. Hayward, *Class. Quant. Grav.* **15**, 3147 (1998).
- [42] H. Kodama, *Prog. Theor. Phys.* **63**, 1217 (1980).
- [43] S. A. Hayward, R. Di Criscienzo, L. Vanzo, M. Nadalini, and S. Zerbini, *Class. Quant. Grav.* **26**, 062001 (2009).

- [44] P. Castorina, D. Kharzeev and H. Satz, *Eur. Phys. J. C* **52**, 187 (2007).
- [45] S.W. Hawking and G.F.R. Ellis, *The large scale structure of space-time* (Cambridge University Press, Cambridge, 1973).
- [46] V. Faraoni, *Phys. Rev. D* **84**, 024003 (2011).